Vascular Endothelial Growth Factor A Competitively Inhibits Platelet-Derived Growth Factor (PDGF)-Dependent Activation of PDGF Receptor and Subsequent Signaling Events and Cellular Responses

Steven Pennock and Andrius Kazlauskas

Schepens Eye Research Institute, Massachusetts Eye and Ear Infirmary, Department of Ophthalmology, Harvard Medical School, Boston, Massachusetts, USA

Certain platelet-derived growth factor (PDGF) isoforms are associated with proliferative vitreoretinopathy (PVR), a sight-threatening complication that develops in a subset of patients recovering from retinal reattachment surgery. Although these PDGF isoforms are abundant in the vitreous of patients and experimental animals with PVR, they make only a minor contribution to activating PDGF receptor α (PDGFRα) and driving experimental PVR. Rather, growth factors outside of the PDGF family are the primary (and indirect) agonists of PDGFRα. These observations beg the question of why vitreal PDGFs fail to activate PDGFRα. We report here that vitreous contains an inhibitor of PDGF-dependent activation of PDGFRα and that a major portion of this inhibitory activity is due to vascular endothelial cell growth factor A (VEGF-A). Furthermore, recombinant VEGF-A competitively blocks PDGF-dependent binding and activation of PDGFR, signaling events, and cellular responses. These findings unveil a previously unappreciated relationship between distant members of the PDGF/VEGF family that may contribute to pathogenesis of a blinding eye disease.

Proliferative vitreoretinopathy (PVR) is a blinding disease that occurs in up to 10% of patients recovering from retinal reattachment surgery (16, 23, 52). Rhegmatogenous retinal detachments allow mislocalization of cells (retinal pigment epithelial cells, glial cells, and fibroblasts) into vitreous (11, 12, 16, 52). These cells proliferate, deposit extracellular matrix, and assemble into a membrane that physically associates with the retina. Contraction of this membrane results in redetachment of the retina and loss of vision (11, 36, 58). The only effective treatment option for patients with PVR is to surgically remove the membrane (23).

Mislocalization of cells to vitreous exposes them to a plethora of growth factors and cytokines that promote cellular responses intrinsic to PVR (41). As a result, there has been a substantial effort to catalogue the growth factors and cytokines that are present in vitreous, and to identify those that are associated with development of PVR (4, 6, 7, 12–17, 20, 24, 28, 34, 35, 37, 39, 41, 44, 48). Unlike neovascular eye diseases, which often depend on a single agent (vascular endothelial cell growth factor A [VEGF-A] [1, 38]), multiple growth factors and cytokines are implicated in the pathogenesis of PVR (4, 6, 7, 12–17, 20, 24, 28, 34, 35, 37, 39, 41, 44, 48).

In the context of the most widely used animal model of PVR, platelet-derived growth factor receptor α (PDGFRα) is an essential mediator of retinal detachment, which is the most clinically relevant facet of this disease (3, 29, 31, 62). Consistent with the concept that multiple growth factors contribute to PVR pathogenesis, PDGFRα can be activated by many PDGF isoforms and even growth factors outside of the PDGF family (non-PDGFs) (39, 40, 44). These non-PDGFs seem to be particularly important for PVR pathogenesis because they activate PDGFRα indirectly, which circumvents internalization and degradation of this receptor, events that limit the half-life of activated PDGFRα. Consequently, the indirect route by which non-PDGFs activate PDGFRα results in a chronically engaged PDGFRα that triggers a unique set of signaling events that promote cellular events intrinsic to PVR (45).

Although a vast body of evidence supports the concept that

ligands are selective for their receptors, ligand specificity within some ligand/receptor families is less than absolute. Such is the case with the ErbB family neuregulins 1 and 2, either of which can bind ErbB-3 or ErbB-4 receptors (47), or the promiscuous interactions between corresponding subclasses of ephrins and Eph receptors (26, 27). Another example of shared receptors has been reported for VEGF-A and PDGF, distantly related members of the cysteine-knot superfamily. Although both growth factors have well-defined receptor partners, VEGF-A binds to PDGFRs on mesenchymal stem cells (5). This finding is consistent with the similarity in overall crystal structure of PDGF-B and VEGF-A (50).

In this report, we addressed the mystery of why PDGF present in vitreous was not able to effectively activate PDGFRα (39). We found that while vitreal PDGFs were functional, vitreous contained inhibitors of PDGF-dependent activation of PDGFRα. We identified VEGF-A as a major contributor to this inhibitory activity. By binding to monomeric PDGFRα, VEGF-A thwarted PDGF-mediated dimerization and activation of this receptor, as well as subsequent signaling events and cellular responses.

MATERIALS AND METHODS

Growth factors, antibodies, and major reagents. Recombinant human PDGF-A, PDGF-AB, PDGF-B, and basic fibroblast growth factor (bFGF) were purchased from Peprotech, Inc. (Rocky Hill, NJ), while recombinant human PDGF-C and PDGF-D were purchased from R&D Systems, Inc. (Minneapolis, MN). VEGF-A (VEGF-165) was obtained from three sources (Peprotech, R&D Systems, and the National Cancer Institute) and
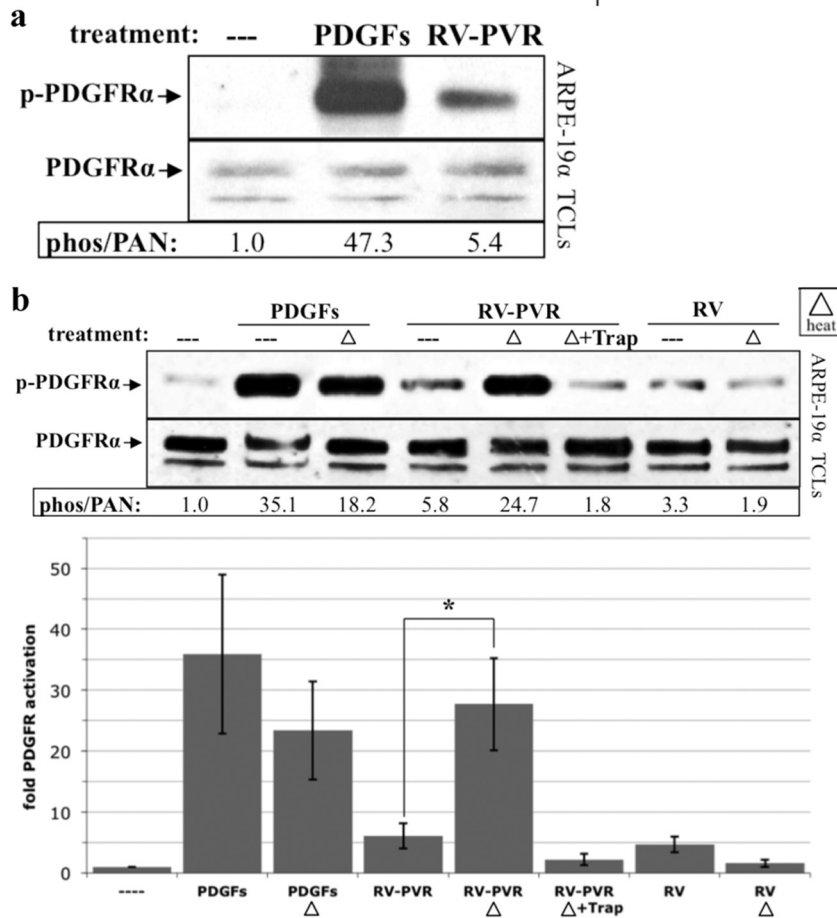
FIG 1 Vitreal PDGFs were inhibited by a heat-labile agent. (a) PVR vitreous activated PDGFRα poorly. ARPE-19α cells, which stably express PDGFRα and induce experimental PVR (42), were grown to near confluence and serum starved overnight. The cells were then treated with serum-free medium alone (—), PDGFs totaling 75 ng/ml (comprising the A, AB, and B isoforms at 40, 30, and 5 ng/ml, respectively, which reflects the composition of PDGFs in PVR vitreous) (39), or vitreous (0.2 ml) from rabbits with PVR (RV-PVR). After 5 min of incubation at 37°C, cells were lysed, and the resulting total cell lysates (TCLs) were subjected to anti-phospho-PDGFRα (pTyr720 and pTyr742) and then anti-PDGFRα Western blot analysis. The resulting signal intensities were quantified. The phospho-PDGFRα immunoblot signal was normalized to total PDGFRα and is presented as the fold induction over the nonstimulated control. There was a statistically significant difference ($P < 0.05$ using a paired t test) between the values obtained from treatment with PDGFs and RV-PVR for three independent experiments. Since RV-PVR contains the same amount and type of PDGFs that were used in the second lane, we conclude that vitreal PDGFs underperformed in their ability to activate PDGFRα. (b) Endogenous PDGFs in PVR vitreous were functional. ARPE-19α cells were cultured and starved as described for panel a. PDGFs totaling 75 ng/ml (same mix as Fig. 1a), RV-PVR (0.2 ml), or vitreous from healthy rabbits, which contains no PDGFs (RV, 0.2 ml) (39) were left unheated (—) or heat treated (△) to 90°C for 5 min and then rapidly cooled on ice. Some of the RV-PVR heat-treated samples were subsequently incubated with 2 μM TRAP. The resulting samples were used to stimulate cells; serum-free media (—) and unheated 75-ng/ml PDGFs were the negative and positive controls, respectively. After a 5-min incubation at 37°C, the cells were lysed, and the resulting TCLs were subjected to the same Western analysis and quantification as for panel a. The bar graph shows the mean fold induction values ± the standard deviations (SD) obtained for three independent experiments (*, $P < 0.05$ using a paired t test). Approximately 50% of the PDGFs used for treatment withstood the heat treatment. Heat treatment increased the ability of RV-PVR to activate PDGFRα, suggesting there is a heat-labile inhibitor in the vitreous that prevents PDGF from activating its receptor.

separately tested to confirm identical inhibitory function. Optimal inhibition by VEGF-A was obtained when using freshly prepared VEGF-A (from lyophilized powder) or −80°C aliquots thawed only once.

The following antibodies were raised in the lab as referenced: anti-PDGFRα (39, 57), anti-phospho-PDGFRα (Y742) (43), anti-PDGFRβ (33), anti-phospho-PDGFRβ (Y751 and Y857) (33), anti-RasGAP (33), and anti-VEGFR2 (54). Anti-phospho-VEGFR2 (Y1175), anti-Axl (C2B12), anti-Akt (9272S), and anti-phospho-Akt (pS473, 9271L) were purchased from Cell Signaling (Danvers, MA), while anti-phospho-PDGFRα (pY720), anti-VEGF-A (A-20), anti-p53 (sc-126), PrA-agarose beads (sc-2001), and horseradish peroxidase (HRP)-conjugated goat anti-rabbit and goat anti-mouse IgG secondary antibodies were purchased from Santa Cruz Biotechnology (Santa Cruz, CA). The enhanced chemiluminescent substrate for HRP detection, the cell sur-

face protein isolation kit (EZ-link Sulfo-NHS-SS-Biotin), and the BS3 cross-linker ($C_{16}H_{18}N_2Na_2O_{14}S_2$) were purchased from Pierce (Rockford, IL). Cycloheximide was purchased from Sigma (St. Louis, MO). TRAP, a chimera consisting of the extracellular domain of PDGFRα fused to human IgG Fc5, was generously provided by Debra Gilbertson at ZymoGenetics (57). Cycloheximide was purchased from Sigma. The VEGFR tyrosine kinase inhibitor II, which blocks both VEGFR1 and VEGFR2 kinases (50% inhibitory concentrations [IC_{50}s] of 180 and 20 nM, respectively), was obtained from Calbiochem (catalog no. 676481). Anti-VEGF-A (Bevacizumab) and the anti-VEGFR1/Flt-1 antibody were gifts from Pat D'Amore at our institute.

Cell culture. ARPE-19α cells are ARPE-19 cells (from the American Type Culture Collection [ATCC], Manassas, VA) overexpressing human PDGFRα, as described previously (39). PAE/KDR cells are pig aortic en-
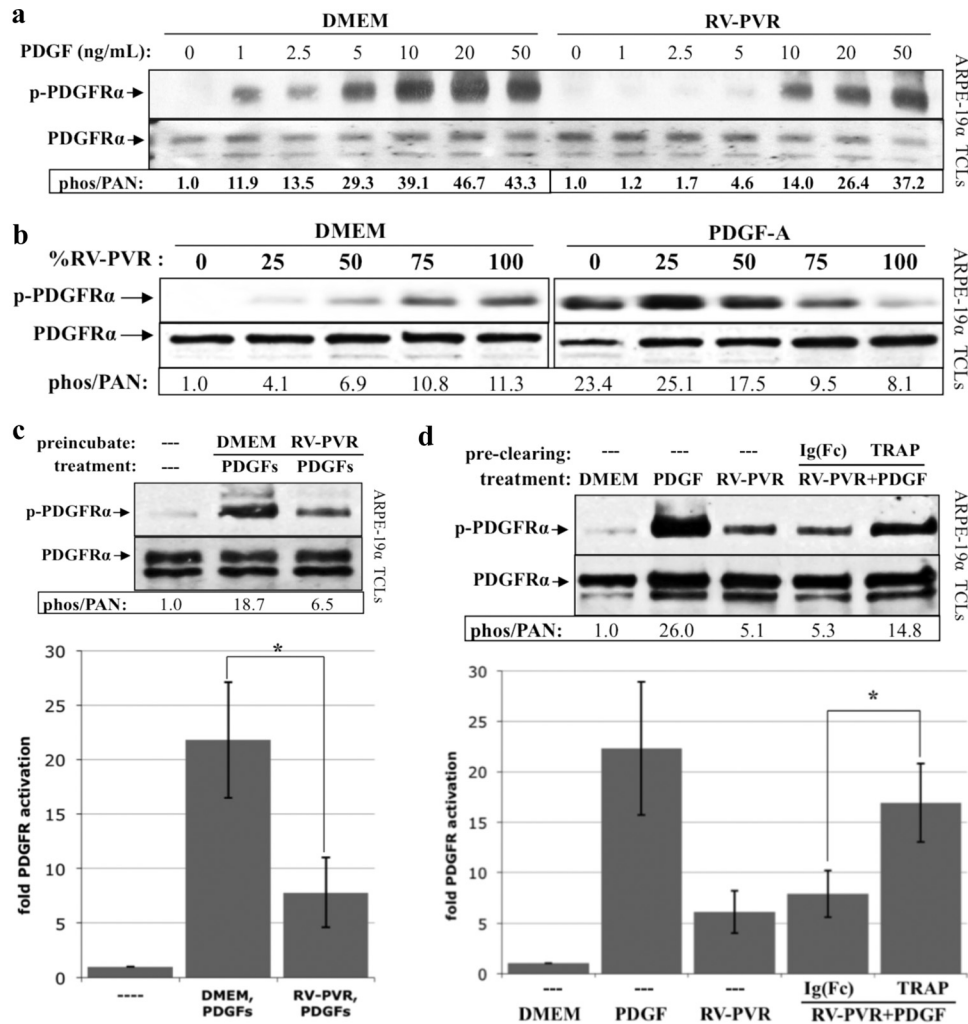
FIG 2 PVR vitreous inhibited PDGF-dependent activation of PDGFRα. (a and b) PDGFRα activation mediated by exogenous PDGF was inhibited by PVR vitreous. ARPE-19α cells were cultured and starved as described for Fig. 1. (a) The indicated amount of PDGF-A was added to either DMEM or RV-PVR, and the resulting solutions were added to cells for 5 min at 37°C. A concentration of 10 ng of VEGF-A/ml corresponds to 0.26 nM. (b) Alternatively, cells were treated with either DMEM or 2.5 ng of PDGF-A/ml in the presence of increasing doses of RV-PVR (DMEM was used as a diluent) for 5 min at 37°C. After treatment, the cells were lysed, and the resulting TCLs were subjected to Western analysis and quantification as described for Fig. 1. The results from three independent experiments for each analysis (a and b) revealed that RV-PVR caused a statistically significant ($P < 0.05$ using a paired t test) decline in PDGFRα phosphorylation at 1, 2.5, 5, and 10 ng of PDGF-A/ml; likewise, RV-PVR titrations greater than 75% of the total treatment volume inhibited PDGF-A-mediated PDGFRα phosphorylation. (c) Cells preconditioned with PVR vitreous were desensitized to subsequent PDGF treatment. ARPE-19α cells, cultured and starved as described in Fig. 1, were either preincubated for 15 min at 37°C with DMEM or RV-PVR (0.2 ml). After incubation, medium or vitreous was removed, and the cells were washed extensively and then treated with serum-free medium alone (—) or supplemented with 10 ng of PDGF-A/ml for 5 min at 37°C. After treatment, the cells were lysed, and the resulting TCLs were subjected to the same Western analysis and quantification as described for Fig. 1. The bar graph shows the mean fold induction of PDGFRα phosphorylation ± the SD obtained for three independent experiments (*, $P < 0.05$ using a paired t test). These results suggest that PVR vitreous contains PDGFRα-associated agents that prevent PDGF-dependent activation of PDGFRα. (d) Preclearing PVR vitreous with the Fc-extracellular domain PDGFRα fusion protein (TRAP) significantly reduced its ability to inhibit PDGF-dependent PDGFRα activation. RV-PVR (0.2 ml) was either left untouched or precleared with 2 μM TRAP or a 2 μM concentration of control IgG-Fc fragment [Ig(Fc)]. The resulting samples were used to stimulate cells; serum-free media (DMEM) and 10 ng/ml of PDGF-A (PDGF) were the negative and positive controls, respectively. After 5 min treatment at 37°C, cells were lysed and the resulting TCLs subjected to the same Western analysis and quantification as in (a). The bar graph shows the mean fold induction values ± the SD obtained for three independent experiments (*, $P < 0.05$ using a paired t test). The ability of TRAP to reduce the inhibitory activity of the vitreous suggests the vitral inhibitors can associate with the extracellular domain of PDGFRα.

dothelial (PAE) cells that overexpress human VEGFR2, as described previously (61). Both cell types were maintained in a 1:1 mixture of low-glucose-containing Dulbecco modified Eagle medium (DMEM; Gibco-BRL) and Ham F-12 medium (Gibco-BRL), supplemented with 10% fetal bovine serum (FBS), 500 U of penicillin/ml, and 500 μg of streptomycin/ml. Fα and Fβ cells are immortalized fibroblasts derived from mouse embryos nullizgous for both PDGFR isoforms (F cells), in which PDGFRα is re-expressed (or PDGFRβ in the case of Fβ cells) (3, 40); Fα cells were used in binding studies and in the dimerization assays (see Fig. 4). Primary mouse embryonic fibroblasts (MEFs) were obtained at third passage from the ATCC. Fα, Fβ, and MEF cells were maintained in high-glucose-containing DMEM (Gibco-BRL) supplemented with 10% FBS, 500 U of penicillin/ml, and 500 μg of streptomycin/ml. All cells were incubated and treated at 37°C in a humidified 5% CO_2 atmosphere.
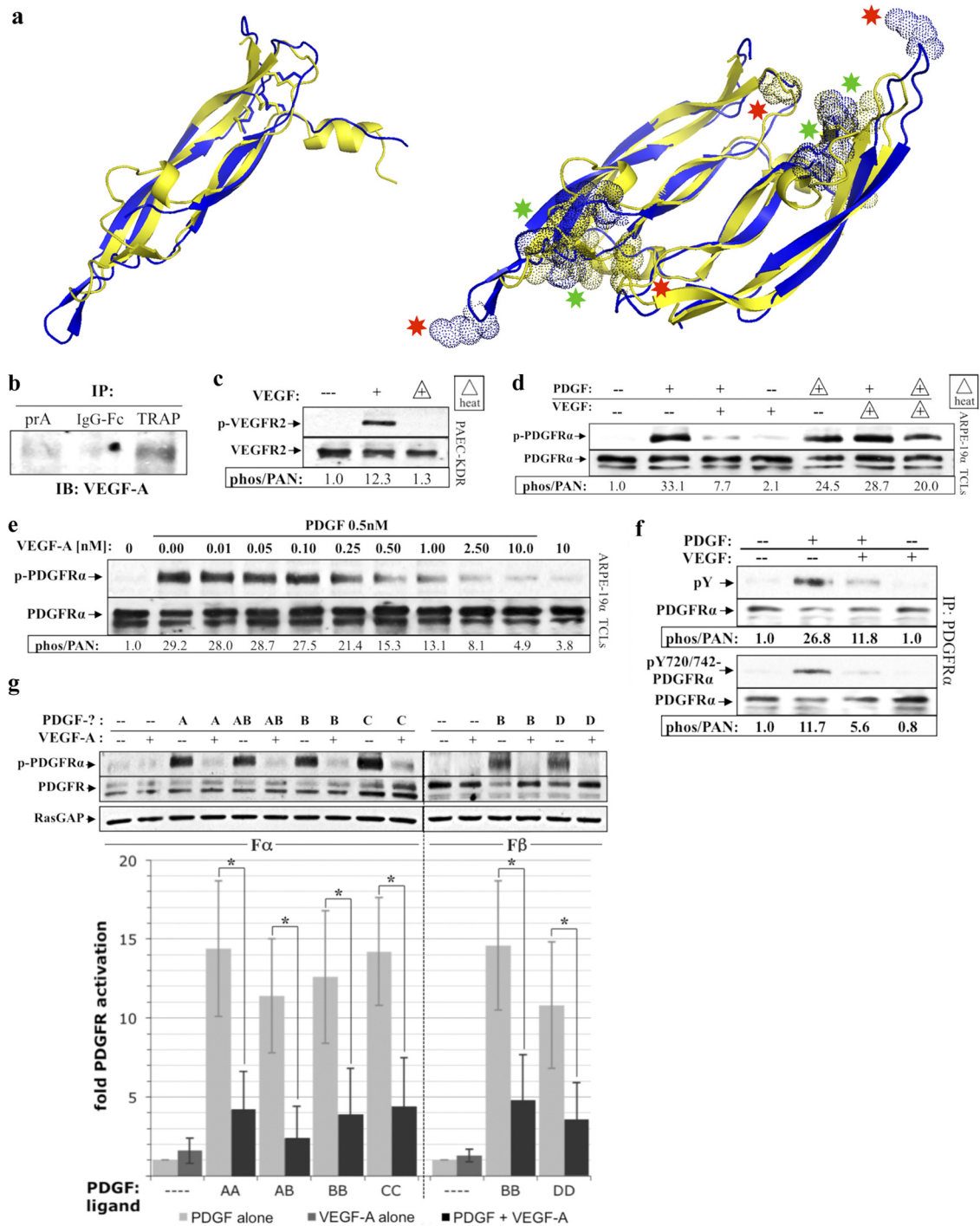
FIG 3 VEGF-A was present in PVR vitreous and inhibited PDGF-dependent activation of PDGFRα. (a) Ribbon structural alignments of human PDGF-B (blue) and human VEGF-A (yellow) crystal structures. Monomers (left) superimpose with a root mean square (RMS) deviation from ideal geometry of 1.7 Å, and dimers (right) superimpose with an RMS deviation of 1.9 Å, indicating that the dimerization modes and overall conformations are very similar (49). Dotted spheres shown on the aligned dimer structures (right) depict areas where the color-matched ligand is thought to make important contacts with its cognate receptor. Both ligands share an equivalent receptor-binding face (depicted above the plane of the paper) containing substantial areas of overlap in their respective receptor-binding regions (green asterisks), as well as receptor-binding regions unique to each ligand (red asterisks). Crystal structures were obtained from PDB depositions of human PDGF-B resolved to 3 Å with accession code 1PDG (51), and human VEGF-A resolved to 1.93 Å with accession code 2VPF (49). Structural alignments were performed using PYMOL software. (b) VEGF-A was recoverable from PVR vitreous using the extracellular domain of PDGFRα. Protein A-agarose (PrA) alone or PrA loaded with either the IgG-Fc fragment (2 μM) or TRAP (2 μM) was incubated with RV-PVR overnight. The matrix was washed extensively, and the retained proteins were eluted with sample buffer and subjected to anti-VEGF-A Western analysis. (c) VEGF's ability to activate VEGFR2 was heat labile. PAE cells overexpressing VEGFR2 (PAE/KDR) were cultured and starved as described for ARPE-19α (Fig. 1). The cells were treated with DMEM alone (—) or 0.5 nM VEGF-A that was unheated (+) or heat treated (+ with triangle outline) to 90°C for 5 min and then rapidly cooled on ice. After treatment for 10 min at 37°C, the cells were lysed and subjected to Western analysis with anti-phospho-VEGFR2 and anti-VEGFR2. The phospho-VEGFR2 immunoblot signal

Cell treatment. Nearly confluent cells were serum starved overnight and treated the next morning. Treatment was carried out under the same conditions in which cells were incubated (37°C in a humidified 5% CO_2 atmosphere). For vitreal treatments, vitreous was added directly to cells after the removal of media and phosphate-buffered saline (PBS) washes. All treatment solutions, including those containing vitreous, were heated to 37°C immediately prior to treatment. Heat-treated solutions (i.e., heated for 5 min at 90°C) were first allowed to rapidly cool on ice and then heated to 37°C prior to treatment.

Preparation of rabbit vitreous (RV). Vitreous was obtained from eyes of either PVR-positive (RV-PVR), or control (RV) rabbits. The animals were sacrificed, the eye were enucleated and frozen. While still frozen, the vitreous was quickly dissected, thawed at room temperature, and centrifuged at 4°C for 5 min at 10,000 × g, and the resulting clarified supernatants were used for all subsequent analyses. Vitreous used for treating cells was always an equal-volume mix of several rabbits of comparable clinical status.

Protein sample preparation and Western blot analysis. (i) Preparation of TCLs. After treatment, cells were washed in ice-cold phosphate-buffered saline (PBS) two times and then lysed by the addition of SDS-PAGE sample buffer (50 mM Tris-HCl [pH 6.8], 10% glycerol, 2% SDS, 1% β-mercaptoethanol, 10 mM EDTA, 0.02% bromophenol blue). Total cell lysates (TCLs) were incubated on ice 20 min, heated to 95°C for 5 min, and then clarified by centrifugation at 13,000 × g, 4°C for 15 min.

(ii) Preparation of PDGFRα immunoprecipitates. Following treatment, cells were washed in ice-cold phosphate-buffered saline (PBS) two times and then lysed in extraction buffer (10 mM Tris-HCl [pH 7.5], 5 mM EDTA, 50 mM NaCl, 50 mM NaF, 1% Triton X-100, 20 μg of aprotinin/ml, 2 mM Na3VO4, and 1 mM phenylmethylsulfonyl fluoride). Lysates were clarified by centrifugation at 13,000 × g, 4°C for 15 min, and PDGFRα was immunoprecipitated from the lysates as previously described (40) using the anti-PDGFRα rabbit polyclonal antibody mentioned above.

(iii) SDS-PAGE and Western blot analysis. TCLs and immunoprecipitates were run on an SDS–7.5% PAGE gel (or SDS–12% PAGE for anti-VEGF-A immunoblots of TRAP-precipitated proteins). Each immunoblot presented here is representative of three independent experiments. Signal intensity was determined by densitometry using Quantity One (Bio-Rad), standardized to background, and then normalized for loading.

(iv) Nondenaturing preparation of proteins and native PAGE. After treatment, the cells were collected in homogenization buffer containing no detergents or reducing agents (0.25 M sucrose, 20 mM Tris-HCl [pH 7], 1 mM MgCl₂, 4 mM NaF, 0.5 mM Na₃VO₄, 20 μg of aprotinin/ml, 0.02% NaN₃, 1 mM phenylmethylsulfonyl fluoride) and homogenized on ice. Homogenates were added 1:1 to 2× acetic acid electrophoresis gel buffer (final concentration of 50 mM acetic acid at pH 5, matching the isoelectric point of monomeric PDGFR). Solubilized homogenates were then clarified at 2,000 × g for 5 min and run on a 7.5% acetic acid nondenaturing polyacrylamide gel using native protein standards. Bromophenol blue was added to each lane as an anionic mobility marker. Semidry transfer and Western blot analysis proceeded as normal.

TRAP affinity purification and MS analysis. The inhibitory activity was isolated from PVR vitreous using a TRAP affinity column. TRAP (2 μM) or a control IgG-Fc fragment (2 μM) were first cross-linked to PrA-agarose beads (200 μl) using 10 mM BS³ (bis[sulfosuccinimidyl]suberate) (Thermo Scientific) for 1 h. Cross-linking was performed in order to eliminate signal masking of low-abundance proteins by the affinity reagents during mass spectrometric (MS) analysis. Chemical modification of TRAP by cross-linking did not compromise its ability to remove inhibitory activity from PVR vitreous or its ability to bind and neutralize PDGFs (data not shown).

PVR vitreous (2 ml) was added to cross-linked TRAP-PrA or IgG-Fc-PrA affinity complexes and incubated overnight at 4°C. Columns were then washed six to eight times with cold PBS and proteins were eluted in a buffer containing 1% SDS and 2.5 mM dithiothreitol. The eluted proteins were digested with trypsin and subjected *en masse* to MS/MS peptide analysis at the Beth Israel Deaconess Medical Center. To identify proteins, the peptide patterns were referenced over multiple databases. After accounting for nonspecific binding (by subtracting IgG-Fc-associated proteins), the proteins remaining included PDGF-A, -B, and -C, confirming that TRAP could purify vitreal proteins.

Receptor competition and ligand binding assays. Receptor competition assays were carried out based on previously described methods (8, 19). Briefly, Fα cells were grown in 24-well plates until nearly confluent and then starved of serum overnight. Cells were then incubated with 0.15 nM ¹²⁵I-PDGF-BB (Perkin-Elmer) in the presence of increasing amounts of PDGF-B, VEGF-A (freshly prepared from lyophilized powder or stored at −80°C and thawed only once), VEGF-A* (stored for >1 week at 4°C, and/or subjected to multiple freeze-thaw cycles), or bFGF. All dilutions were made with binding buffer (DMEM with 0.2% bovine serum albumin [BSA] and 20 mM HEPES [pH 7.2]). Cells were incubated for 2 h at 4°C and then washed extensively with cold binding buffer. After incubation, cells from each well were harvested using 200 μl of 1% Triton X-100 extraction buffer, incubated for 5 to 10 min at 4°C, and finally counted using a gamma counter to determine the amount of ¹²⁵I-PDGF-BB bound.

¹²⁵I-PDGF-BB ligand binding assays were performed as described

was normalized to the total VEGFR2; the results are presented as the fold induction over the nonstimulated control. (d) VEGF-A-mediated inhibition of PDGF-dependent activation of PDGFRα was heat labile. ARPE-19α cells were cultured and starved as described for Fig. 1. The cells were treated with DMEM alone (—), 0.5 nM PDGF-A, 0.5 nM VEGF-A, or both 0.5 nM PDGF-A and 0.5 nM VEGF-A for 10 min at 37°C. . . ." OK as edited? If not, pls. clarify.>. Samples indicated by triangles were heat treated and then rapidly cooled on ice. After treatment, the cells were lysed and subjected to Western analysis with anti-phospho-PDGFRα and anti-PDGFRα. Heat treatment eliminated VEGF-A's ability to inhibit PDGF-mediated activation of PDGFRα. (e) PDGF-mediated activation of PDGFRα was inhibited by VEGF-A. The indicated concentrations of VEGF-A were added to DMEM containing 0.5 nM PDGF-A or to DMEM alone. ARPE-19α cells, prepared as described in the legend of Fig. 1, were treated with the resulting solutions for 10 min at 37°C, lysed and analyzed by Western analysis as in Fig. 1. The fold induction values of PDGFRα activation are given below the blot. The results from three independent experiments revealed that VEGF-A and PDGF-A had similar affinities for PDGFRα. 0.5 nM PDGF is 14 ng/ml; 0.5 nM VEGF-A is 19 ng/ml. (f) VEGF-A inhibited global tyrosine phosphorylation of PDGFRα. Serum-starved ARPE-19α at 75% confluence was treated with DMEM alone (—), 0.5 nM PDGF-A, 0.5 nM VEGF-A, or both 0.5 nM PDGF-A and 0.5 nM VEGF-A for 10 min at 37°C. After treatment, the cells were lysed, and the clarified lysates were immunoprecipitated using anti-PDGFRα, followed by Western analysis with antibodies against PDGFRα, all phosphotyrosines on PDGFRα (pY), or a combination of antibodies against specific PDGFRα phospho-sites at Y720 and Y742 (pY720/742-PDGFRα). Phospho-PDGFRα immunoblot signals were normalized to total PDGFRα; the results are presented as the fold induction over the nonstimulated control for each pair. (g) VEGF-A competed with all PDGF isoforms for activation of their respective PDGFRs. Serum-starved cells that exclusively expressed either PDGFRα (Fα) or PDGFRβ (Fβ) were treated for 10 min at 37°C with either DMEM (—) or a 0.5 nM concentration of the indicated PDGF isoform in the absence or presence of equimolar amounts of VEGF-A (0.5 nM). After treatment, the cells were lysed, and the resulting TCLs were subjected to Western analysis with antibodies against phospho-PDGFR (anti-pTyr720 and pTyr742 for PDGFRα; anti-pTyr751 and pTyr857 for PDGFRβ), followed by anti-PDGFR(α or β) and anti-RasGAP to normalize protein loading. Immunoblot signals were quantified as described in Fig. 1. The bar graph underneath shows the mean percent inhibition ± the SD of PDGFRα and PDGFRβ activation observed for three independent experiments (*, $P < 0.05$ using a paired t test). Light gray bars represent DMEM or PDGF treatment in the absence of VEGF-A, dark gray bars represent VEGF-A (0.5 nM) treatment alone, and black bars represent PDGF treatment in the presence of 0.5 nM VEGF-A. These data indicate that VEGF-A comparably inhibited all PDGF isoforms from activating their respective PDGFR(s).
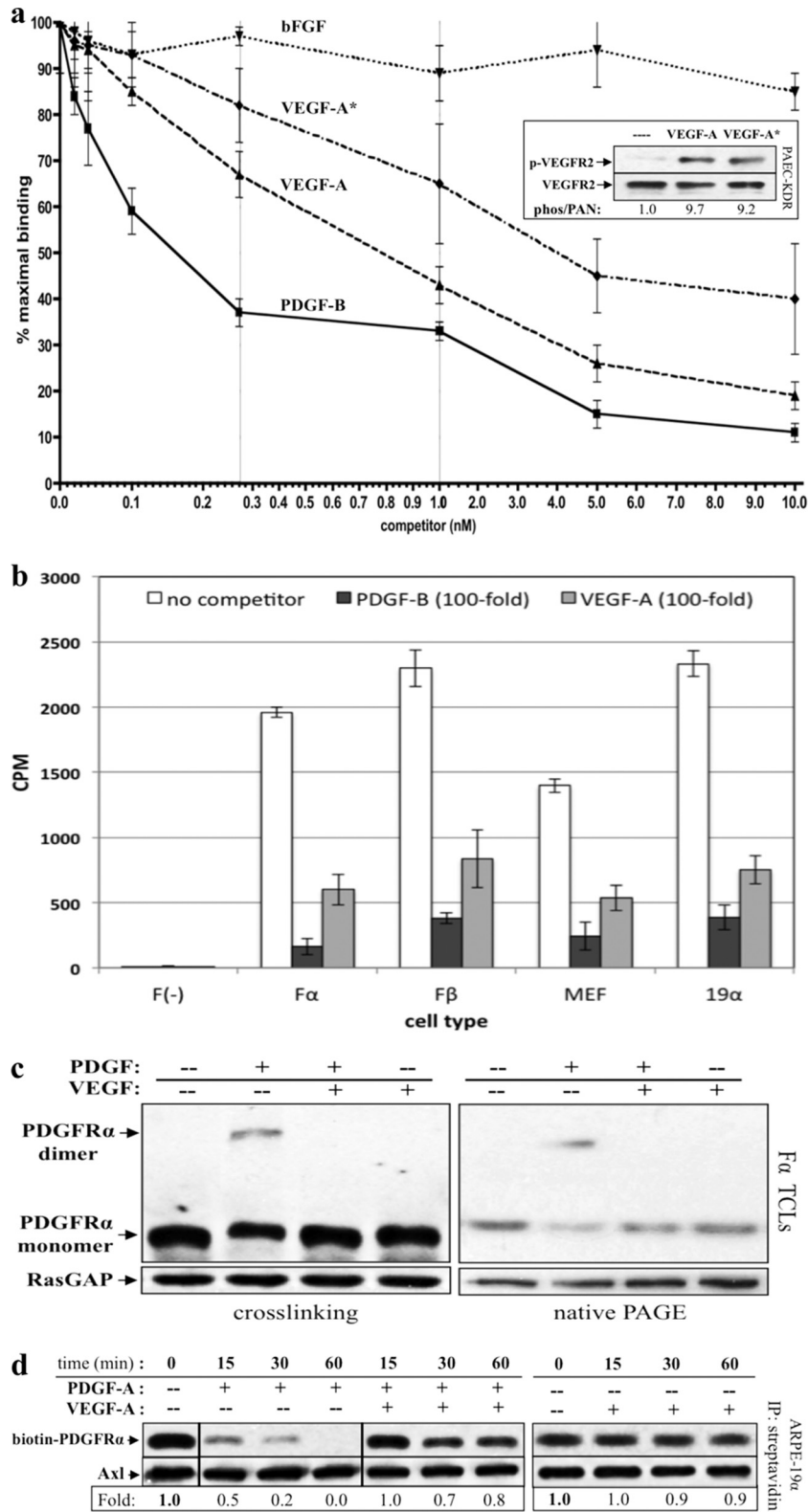
FIG 4 VEGF-A bound to PDGFRα and prevented PDGF-dependent dimerization and internalization. (a) VEGF-A competes with PDGF-B in a dose-dependent manner for binding to PDGFRα. Fα cells were grown in 24-well plates until nearly confluent, serum starved, and subsequently incubated with 0.15 nM ^{125}I-PDGF-B in the presence of increasing amounts of unlabeled PDGF-B, VEGF-A (freshly prepared from lyophilized powder), VEGF-A* (stored for >1 week at 4°C and/or subjected to multiple freeze-thaw cycles), or bFGF. The cells were incubated for 2 h at 4°C and then washed extensively with cold binding buffer. After incubation, the cells were harvested, and the radioactivity was quantified by using a gamma counter to determine the amount of ^{125}I-PDGF-BB bound. The resulting IC$_{50}$s were 0.16 ± 0.03 nM for PDGF-B and 0.78 ± 0.13 nM for VEGF-A. Thus, VEGF-A binds to PDGFRα with a 5.2-fold-lower affinity than its cognate

above but using F, Fα, Fβ, MEFs, or ARPE-19α cells with 0.15 nM ^{125}I-PDGF-BB plus binding buffer alone or a 100-fold excess (15 nM) of unlabeled PDGF-B or VEGF-A.

Receptor dimerization assay. Fα cells grown in six-well plates were allowed to reach 75% confluence, starved of serum overnight, and then treated as shown in Fig. 4c. After treatment, cells were washed with ice-cold PBS and incubated with 2 mM BS^3 cross-linker solution for 30 min at 4°C with mild agitation. The cross-linking reaction was terminated by addition of 20 mM Tris for 5 min at room temperature. After two washes with ice-cold PBS, the cells were lysed in extraction buffer (10 mM Tris-HCl [pH 7.4], 5 mM EDTA, 50 mM NaCl, 50 mM NaF, 1% Triton X-100, 20 μg of aprotinin/ml, 2 mM Na$_3$VO$_4$, 1 mM phenylmethylsulfonyl fluoride). The lysates were clarified by 4°C centrifugation at 13,000 × g for 15 min, run on 8% SDS-PAGE, and subjected to Western blot analysis with anti-PDGFRα antibody. To assess dimerization without cross-linking, Fα cells were prepared and treated as described above, after which, the cells were collected in homogenization buffer and prepared as described in the "Nondenaturing preparation of proteins and native PAGE."

Receptor internalization assay. ARPE-19α cells grown in six-well plates were allowed to reach 75% confluence, serum starved overnight, pretreated with 2 mM cycloheximide for 30 min, and then treated as described for Fig. 4d. After treatment, cell surface proteins were isolated according to the instructions provided by the cell surface protein isolation kit (Pierce). In brief, the cells were washed with PBS and incubated with 0.25 mg of Sulfo-NHS-SS-Biotin/ml (in PBS) for 1 h at 4°C with mild agitation. Biotinylation of cell surface proteins was terminated by briefly adding quenching solution. The cells were washed twice with PBS, extraction buffer was added, and the plates were rocked at 4°C for 30 min. The lysates were clarified by 4°C centrifugation at 13,000 × g for 15 min. Biotinylated proteins (i.e., those remaining on the cell surface at the end of treatment) were precipitated with NeutrAvidin-agarose beads for 1 h, followed by five washes with extraction buffer. NeutrAvidin-agarose-bound proteins were eluted in sample buffer and subjected to SDS–8% PAGE, followed by Western blot analysis with antibodies against PDGFRα and Axl (the latter as a biotinylated loading control).

Cell contraction assay. The cell contraction assay relates to the pathological process whereby vitreal cells in the ERM to exert traction on the retina (causing detachment) and is one way to assess the effects of various treatments on the contractility of cells. The assay was performed as previously described (22, 30). Briefly, a cell suspension was prepared containing 1.5 mg of neutralized collagen I at pH 7.2 (INAMED, Fremont, CA)/ml and 10^6 cells/ml and transferred to a 24-well plate preincubated with PBS plus 5 μg of BSA/μl for at least 6 h. Collagen gels solidified upon

incubation at 37°C for 90 min. After this, the gels were overlaid with 0.5 ml of DMEM or DMEM plus whatever treatment was used. Medium containing the desired treatment was changed daily. The gel diameter was measured on days 0, 1, 2, and 3. At day 0, the diameter of the gel equals the diameter of the well. Triplicates were performed in each experiment. For each assay, no fewer than two independent experiments were performed.

Statistical data analysis. Data were analyzed using the unpaired t test. A P value of <0.05 was considered statistically significant.

RESULTS

PVR vitreous inhibited PDGF-dependent activation of PDGFRα. PVR vitreous contains high levels of those PDGF isoforms, which activate PDGFRα, and yet PDGF-responsive cells treated with PVR vitreous activate PDGFRα poorly (44). As seen in Fig. 1a, the degree of PDGFRα activation shown by cells treated with PVR vitreous was <15% of that observed in cells treated with the same amount and composition of PDGFs in the absence of vitreous. In light of the unusually high thermostability of certain PDGF isoforms (55), we tested whether heating vitreous could improve the potency of vitreal PDGFs. Heat-treated vitreous activated PDGFRα better, and this improvement was PDGF dependent, i.e., neutralizing PDGFs blocked this response (Fig. 1b). These findings indicate that vitreal PDGFs were capable of activating PDGFRα and suggested that vitreous contained a heat-labile inhibitor of this event.

If vitreous contained an inhibitor that prevented vitreal PDGFs from activating PDGFRα, then it may also inhibit the ability of exogenous PDGF to perform this function. Indeed, RV-PVR suppressed PDGFRα activation driven by exogenously administered recombinant human PDGF, especially at lower doses (Fig. 2a). Furthermore, increasing the concentration of vitreous overcame activation of PDGFRα by a fixed dose of recombinant PDGF (Fig. 2b). These observations suggested that vitreous contains an agent or agents that competitively blocks PDGF-dependent activation of PDGFRα.

To assess whether the putative inhibitor was acting at the level of PDGF or PDGFRα, we preincubated cells (i.e., their receptors) with RV-PVR, and after its removal, challenged these cells with recombinant PDGF. PDGF-dependent activation of PDGFRα was attenuated in RV-PVR-pretreated cells (Fig. 2c). This result suggested that the inhibitor acted at the level of PDGFRα. This idea was reinforced by the observation that absorbing RV-PVR

ligand, although this difference remains within the same log order of binding affinity. VEGF-A* bound much more weakly (IC$_{50}$ ~4 nM) whereas bFGF did not compete. The inset shows that both VEGF-A and VEGF-A* stimulated a similar level of phosphorylation of VEGFR2 in PAE-KDR cells. (b) VEGF-A bound to PDGFRs on a variety of cell types. F, Fα, Fβ, MEFs, or ARPE-19α cells were incubated with 0.15 nM ^{125}I-PDGF-B plus binding buffer alone (no competitor) or a 100-fold excess (15 nM) of unlabeled PDGF-B or VEGF-A. No binding was observed for F cells, which do not express PDGFRs, whereas VEGF-A bound to all other cell types: Fα and Fβ cells (expressing PDGFRα and PDGFRβ, respectively) and MEFs and ARPE-19α cells (expressing both PDGFR isoforms). (c) VEGF-A inhibited PDGF-dependent dimerization of PDGFRα. Fα cells were grown to ca. 75% confluence and serum starved overnight. The cells were then treated with DMEM alone (—), 0.5 nM PDGF-A, 0.5 nM VEGF-A, or both 0.5 nM PDGF-A and 0.5 nM VEGF-A for 10 min at 20°C. (Left panel) After treatment, the cells were placed on ice, and proximal cell surface proteins were covalently linked using a membrane-impermeable cross-linker (described in Materials and Methods). Subsequently, cells were lysed and subjected to Western analysis with anti-PDGFRα and anti-RasGAP (to assess protein loading). (Right panel) Alternatively, dimerization was assessed without cross-linking by preparing samples under nondenaturing and nonreducing conditions and performing native PAGE (described in Materials and Methods). The Western analysis was the same as for the left panel. These data indicate that PDGF-mediated dimerization of PDGFRα was inhibited by VEGF-A and that VEGF-A itself was unable to induce this response. (d) PDGF-mediated internalization of PDGFRα was inhibited by VEGF-A. ARPE-19α cells at 75% confluence were serum starved overnight. At 30 min prior to treatment, cycloheximide (2 mM) was added and retained for the duration of the experiment. The cells were then either left untreated (lane 0) or treated for the indicated times with 0.5 nM PDGF-A, 0.5 nM VEGF-A, or both 0.5 nM PDGF-A and 0.5 nM VEGF-A. After treatment, the cells were washed and placed on ice, and the cell surface proteins were biotinylated with sulfo-NHS-SS-biotin for 1 h and then quenched. Subsequently, the cells were lysed and the resulting lysates clarified. Biotinylated proteins (i.e., those remaining on the cell surface at the end of treatment) were precipitated with NeutrAvidin-agarose beads. NeutrAvidin-precipitated proteins were eluted with sample buffer and subjected to Western analysis with anti-PDGFRα and anti-Axl (the latter to assess equal loading of biotinylated proteins). The biotin-PDGFRα signal was normalized to Axl and is presented here as a ratio of the amount of receptor remaining on the cell surface over the amount of receptor remaining of the cell surface in untreated control (i.e., the absence of ligand-induced receptor internalization). The results from three independent experiments reveal that PDGF-A induced rapid internalization of PDGFRα, and this response was attenuated in the presence of an equimolar amount of VEGF-A. VEGF-A alone did not induce PDGFRα internalization.
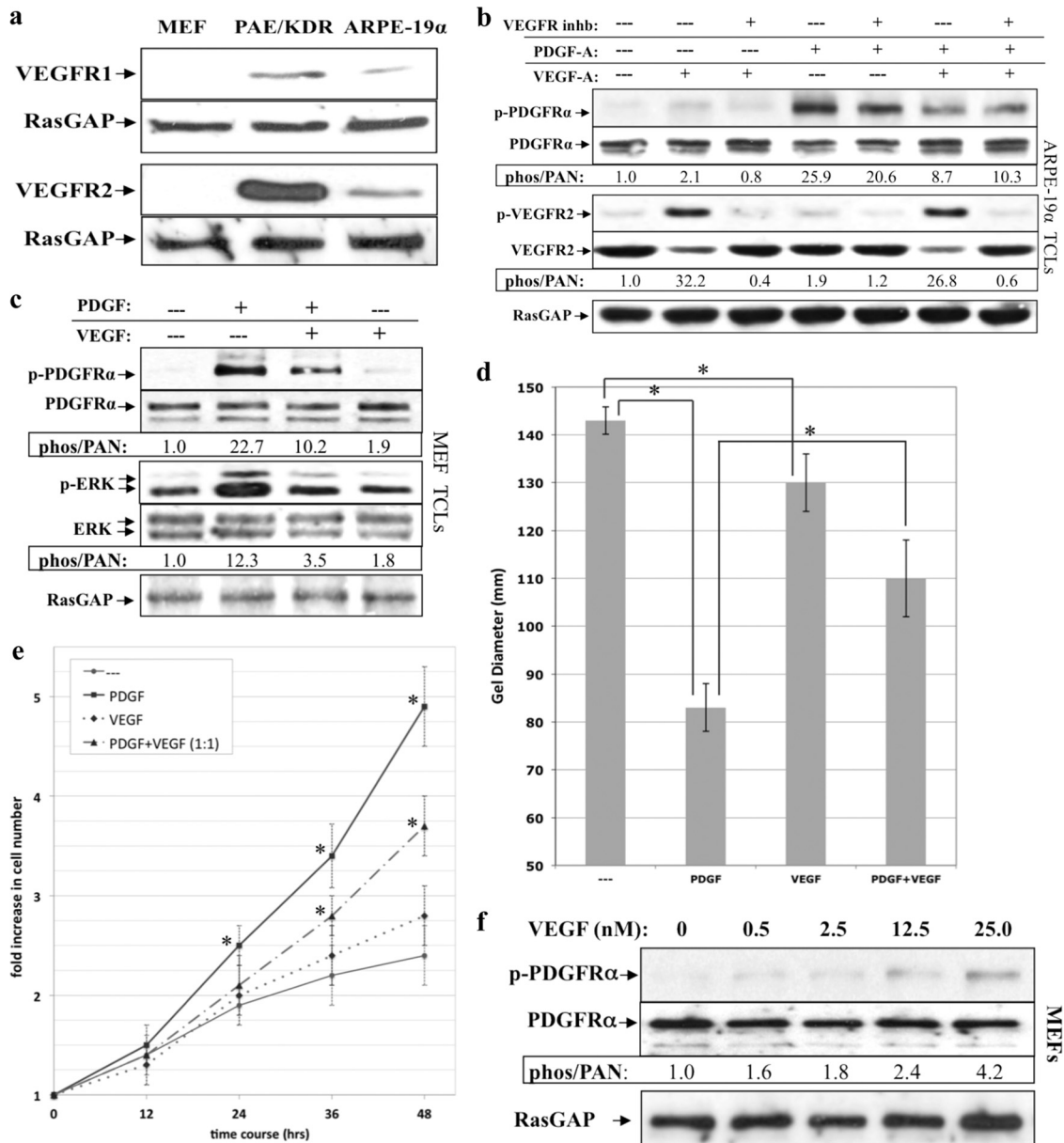
FIG 5 VEGF-A antagonized PDGFRα and PDGF-driven cellular response without engaging VEGFRs. (a) Expression of VEGFR1 and VEGFR2 in MEFs, PAE/KDR, and ARPE-19α cells. MEFs, PAE/KDR, and ARPE-19α cells were cultured in 10% serum to near confluence, lysed, and subjected to Western analysis using anti-VEGFR1, anti-VEGFR2, and anti-RasGAP. MEFs express neither VEGFR isoform, whereas PAE/KDR and ARPE-19α cells express both VEGFR1 and VEGFR2. (b) VEGFR kinase activity was not required for VEGF-A-dependent inhibition of PDGF-driven PDGFRα activation. ARPE-19α cells were cultured and starved as described in Fig. 1. The cells were either left untreated or treated for 10 min with different combinations of PDGF-A (0.5 nM) and VEGF-A (0.5 nM) in either the presence or the absence of a VEGFR tyrosine kinase inhibitor (VEGFR inhb), which was added 30 min prior to treatment, and used at a concentration sufficient to neutralize both VEGFR isoforms (360 nM). After treatment for 10 min at 37°C, the cells were lysed and subjected to Western analysis with anti-phospho-PDGFRα, anti-PDGFRα, anti-phospho-VEGFR2, and anti-VEGFR2. Phospho-PDGFRα and phospho-VEGFR2 immunoblot signals were normalized to total PDGFRα and VEGFR2, respectively; the results are presented as the fold induction over the nonstimulated control for each pair. RasGAP was used to assess equal loading of the protein. These data show that VEGFR kinase does not contribute to VEGF's ability to inhibit PDGF-mediated activation of PDGFRα. (c) VEGF inhibited PDGF-driven activation of PDGFRα-mediated signaling events. Serum-starved MEFs at 75% confluence were treated with DMEM alone (—), 0.5 nM PDGF-A, 0.5 nM VEGF-A, or both 0.5 nM PDGF-A and 0.5 nM VEGF-A for 10 min at 37°C. After treatment, the cells were lysed and subjected to Western analysis with anti-phospho-PDGFRα, anti-PDGFRα, anti-phospho-Erk, and anti-Erk. Phospho-PDGFRα and phospho-Erk immunoblot signals were normalized to total PDGFRα and Erk, respectively; the results are presented as the fold induction over the unstimulated control for each pair. RasGAP was used to assess equal loading of the protein. (d) VEGF-A inhibited PDGF-driven PDGFRα-mediated cell contraction. MEFs were subjected to the collagen gel contraction assay in the presence of DMEM (—), 0.5 nM PDGF-A, 0.5 nM VEGF-A, or both PDGF-A (0.5 nM) and VEGF-A (0.5 nM). The gel diameter was measured manually at day 2, and the data presented are the means of three independent experiments ± the SD (shown as error bars; *, $P < 0.05$ using a paired t test). (e) VEGF-A inhibited PDGF-driven PDGFRα-mediated proliferation. Equal numbers of MEFs (10^5) were seeded on plates and grown to 50% confluence, after which serum-containing media was replaced with DMEM alone or DMEM supplemented with 0.5 nM PDGF-A (PDGF), 0.5 nM VEGF-A (VEGF), or both 0.5 nM PDGF-A and 0.5 nM VEGF-A (PDGF+VEGF). The cells were grown for up to 48 h at 37°C, and the medium was replaced every 24 h with fresh treatment. At the time points indicated, cells from each treatment were counted by hemocytometry. The graph presents data from three independent experiments showing the fold increase in cell number (means ± the SD) normalized to the number of cells initially seeded (*, $P < 0.05$ using a paired t test relative to no-treatment controls at the indicated times). (f) VEGF-A-mediated activation of PDGFRα. The indicated concentrations of VEGF-A were added to serum-starved MEFs at 75% confluence for 10 min at 37°C. The cells were lysed, and the resulting TCLs were subjected to the same Western analysis and quantification as described in Fig. 1. The fold induction values of PDGFRα activation are given below the blots. A concentration of 25 nM VEGF-A corresponds to 955 ng/ml.

with an Ig-Fc fusion protein containing the extracellular domain of PDGFR α (TRAP) reduced its ability to inhibit PDGF-dependent PDGFRα activation (Fig. 2d). These data indicated that the inhibitor acted at the level of PDGFRα. Furthermore, the ability of TRAP to clear vitreous of inhibitory activity pointed to its potential utility as a reagent for purifying and identifying this inhibitor.

VEGF-A inhibited both PDGF-dependent activation and binding to PDGFRα. To isolate putative PDGFRα inhibitors, RV-PVR was passed over a control or TRAP affinity column, and the retained proteins were subjected to MS analysis. Out of the resulting list of potential PDGFRα inhibitors, we focused on VEGF-A because it was structurally similar to PDGF-B (Fig. 3a) (49, 50) and because it is capable of binding to PDGFRs (5). Additional experiments verified the MS data; VEGF-A was selectively recovered with the TRAP affinity matrix (Fig. 3b), was present in RV-PVR (6, 53), and was heat labile (Fig. 3c and d).

To test whether VEGF-A inhibited PDGF-mediated PDGFRα activation, we simultaneously treated cells with PDGF-A and increasing amounts of VEGF-A (Fig. 3e). An equimolar amount of VEGF-A inhibited PDGF-A-dependent activation of PDGFRα by ca. 50%. Furthermore, VEGF-A inhibited global tyrosine phosphorylation, as opposed to a specific subset of tyrosine phosphorylation sites (Fig. 3f). Additional experiments revealed that VEGF-A effectively competed for binding with other PDGF isoforms to either PDGFRα or PDGFRβ (Fig. 3g).

To test whether VEGF-A also prevented binding of PDGF to its receptors, we assessed its ability to compete with ^{125}I-PDGF for binding to fibroblasts expressing PDGFRα. Although not as effective as PDGF-B, VEGF-A specifically blocked this event, whereas another growth factor (bFGF) did not (Fig. 4a). Curiously, VEGF-A began to lose this ability even after 1 week at 4°C (Fig. 4a), whereas it retained its ability to activate VEGFR2 (insert of Fig. 4a). VEGF-A also competed with ^{125}I-PDGF for binding in cells expressing only PDGFRβ or both PDGFRs (Fig. 4b). Consistent with the observation that VEGF-A prevented binding of PDGF, it also blocked PDGF-dependent dimerization (Fig. 4c) and internalization (Fig. 4d) of PDGFRα. In contrast, VEGF-A itself did not induce either of these outcomes (Fig. 4c and d). Taken together, this series of experiments supports the idea that VEGF-A blocked PDGF-dependent activation of PDGFRα by binding and retaining PDGFRα monomers on the cell surface.

VEGF-A attenuated PDGF-dependent activation of PDGFR independently of VEGFRs. The fact that VEGF-A antagonized PDGF-dependent activation of PDGFRs in VEGFR-expressing cells (ARPE-19α, Fig. 5a) raised the possibility that this event involved VEGF receptors (VEGFRs). However, a VEGFR inhibitor did not influence the ability of VEGF-A to suppress PDGF-dependent activation of PDGFRα in ARPE-19α cells (Fig. 5b). Furthermore, VEGF-A antagonized PDGF-dependent activation of PDGFRα in MEFs (Fig. 5c), which did not express detectable levels of VEGFR1 or VEGFR2 (Fig. 5a). We conclude that VEGF-A acts independently of VEGFR1 and VEGFR2 to suppress PDGF-dependent activation of PDGFRα.

VEGF-A antagonized PDGF-driven signaling events and cellular responses. To assess whether VEGF-A also blocked PDGF-driven downstream signaling events and cellular responses, we monitored these outcomes in primary MEFs stimulated with PDGF, VEGF-A, or equimolar amounts of both PDGF and VEGF-A. VEGF-A not only blocked PDGF-driven activation of PDGFRα but also attenuated downstream Erk activation (Fig. 5c).

Moreover, VEGF-A diminished both PDGF-driven contraction of MEFs in a collagen gel (Fig. 5d) and proliferation (Fig. 5e). We conclude that VEGF-A antagonized PDGF-driven signaling events and cellular responses.

Consistent with Ball et al. (5), we observed that VEGF-A activated PDGFRα (Fig. 3d, 3e, 5b, and 5c). The extent of activation was typically very modest, and while a supraphysiological dose (25 nM is 955 ng/ml) of VEGF-A increased the response somewhat (Fig. 5f), it never achieved the level observed with PDGF. We conclude that whereas VEGF-A can activate PDGFRα, it does so poorly in the cell types used here.

VEGF-A determined the mode of PDGFRα activation. Our findings that VEGF-A is the inhibitor present in vitreous predicted that neutralizing it would increase the efficiency of vitreal PDGFs to activate PDGFRα. Indeed, the addition of an anti-VEGF-A antibody to RV-PVR greatly increased its ability to activate PDGFRα, and the potentiation was blocked by TRAP (Fig. 6a).

The implication of this observation is that VEGF-A determines the mode by which PDGFRα will be activated. RV-PVR has a plethora of non-PDGFs, which drive prolonged, indirect activation of PDGFRα (Fig. 6a) (44, 53). Direct activation of PDGFRα antagonizes indirect activation by promoting the rapid clearance of PDGFRα from the cell surface and subsequent degradation (Fig. 4d) (45). Consequently, neutralizing VEGF-A in RV-PVR should promote clearance of PDGFRα from the cell surface because neutralizing VEGF-A will potentiate vitreal PDGFs. This is indeed what we observed (Fig. 6b). These findings indicate that in RV-PVR, VEGF-A sustains cell surface expression of PDGFRα by antagonizing vitreal PDGFs, which promote internalization and degradation of PDGFRα.

Furthermore, by antagonizing PDGF's ability clear PDGFRα from the cell surface, VEGF-A should enable the indirect mode of PDGFRα activation. To test this idea, we compared the impact of VEGF-A on the mode of PDGFRα activation when both types of agonists (PDGF and non-PDGFs) were present. As shown in Fig. 6c, vitreous from healthy rabbits (RV) (which contains only non-PDGFs [39, 53]) induced the signaling events diagnostic of indirect activation of PDGFRα: no change in PDGFRα, prolonged activation of Akt, and suppression of p53. As expected, the addition of PDGF resulted in a decline in the level of PDGFRα and mitigation of these signaling events. Importantly, VEGF-A largely reversed this PDGF-dependent phenomenon. We conclude that in the presence of both types of agonists, VEGF-A ensures that indirect activation of PDGFRα predominates. In the context of PVR, this has profound implications since indirect activation of PDGFRα drives the pathogenesis of this disease (Fig. 6d) (44).

DISCUSSION

Despite their abundance (39) and functionality, PDGFs in PVR vitreous were unable to efficiently activate PDGFRα due to the presence of a heat-labile inhibitor. This inhibitor acted at the level of the receptor and could be isolated from vitreous using a fusion protein that included the PDGFRα extracellular domain. Among the proteins affinity purified in this way, we focused on VEGF-A because of its structural similarity to PDGF and its known ability to bind PDGFRs (5, 50). Like the vitreal inhibitor, purified VEGF-A attenuated PDGF-dependent activation of PDGFRα. VEGF-A's mode of inhibition involved binding to PDGFRs and thereby preventing PDGF-mediated dimerization, activation, and internalization of PDGFRα. Furthermore, VEGF-A attenuated
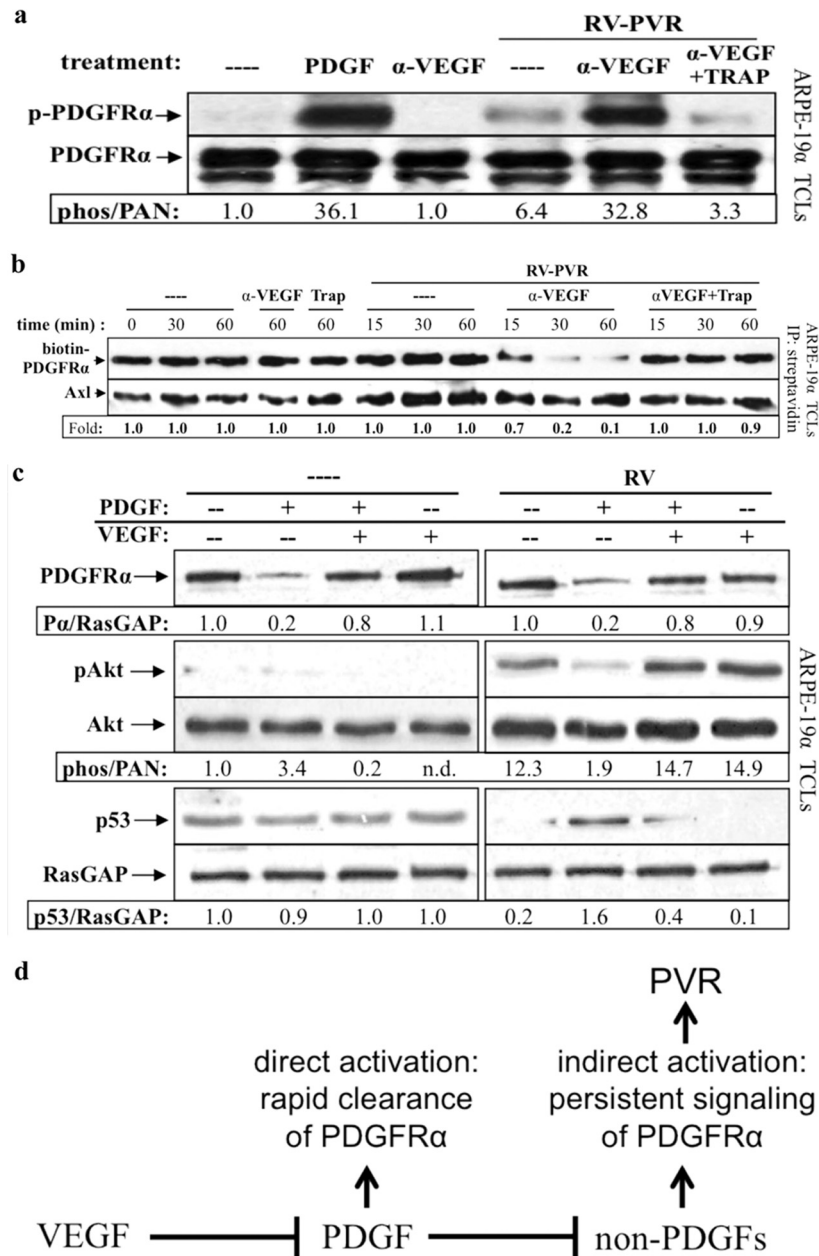
FIG 6 Neutralizing VEGF-A enabled vitreal PDGFs to activate PDGFRα and inhibit its indirect activation by vitreous. (a) Anti-VEGF-A promoted vitreal PDGFs to activate PDGFRα. Serum-starved ARPE-19α cells were treated 10 min at 37°C with buffer alone (–), PDGF-A (0.5 nM), or RV-PVR (0.2 ml) that was either left alone, preincubated 30 min with 25 μg of anti-VEGF-A (α-VEGF)/ml, or preincubated 30 min with 25 μg of anti-VEGF-A/ml, after which 2 μM TRAP was added. After treatment, the cells were lysed, and the resulting TCLs were subjected to the same Western analysis and quantification as described in Fig. 1. These results demonstrate that neutralizing VEGF-A significantly enhanced the ability of endogenous PDGFs in PVR vitreous to activate PDGFRα. (b) Anti-VEGF-A promoted vitreal PDGFs to internalize PDGFRα. ARPE-19α cells at 75% confluence were serum starved overnight. At 30 min prior to treatment, cycloheximide (2 mM) was added and retained for the duration of the experiment. The cells were then either left untreated (—) over the time course or treated for the indicated times in the absence of RV-PVR with 25 μg of α-VEGF-A or 2 μM TRAP/ml or treated for the indicated times in the presence of RV-PVR (0.2 ml) with nothing (—), 25 μg of α-VEGF-A/ml, or 25 μg of α-VEGF-A/ml + 2 μM TRAP. After treatment, the cells were washed and placed on ice, and cell surface proteins were biotinylated with Sulfo-NHS-SS-Biotin for 1 h and then quenched. Subsequently, the cells were lysed, and the resulting lysates were clarified. Biotinylated proteins (i.e., those remaining on the cell surface at the end of treatment) were precipitated with NeutrAvidin-agarose beads. NeutrAvidin-precipitated proteins were eluted with sample buffer and subjected to Western analysis with anti-PDGFRα and anti-Axl (the latter to assess equal loading of biotinylated proteins). The biotin-PDGFRα signal was normalized to Axl and is presented here as a ratio of the amount of receptor remaining on the cell surface over the amount of receptor remaining of the cell surface in the untreated control (i.e., absence of ligand-induced receptor internalization). The results from three independent experiments reveal that VEGF-A helps retain PDGFRα at the cell surface by antagonizing PDGF-A-mediated PDGFRα internalization. (c) Anti-VEGF-A promoted PDGF-induced direct signaling of PDGFRα and attenuated RV-induced indirect signaling responses. Serum-starved ARPE-19α cells at 75% confluence were treated with DMEM alone (—), 0.5 nM PDGF-A, 0.5 nM VEGF-A, or both in the absence (—) or presence of normal rabbit vitreous (RV) for 2 h at 37°C. After treatment, the cells were lysed and subjected to Western analysis with anti-PDGFRα, anti-phospho-Akt, anti-Akt, anti-p53, and anti-RasGAP. PDGFRα and phospho-Akt immunoblot signals were normalized to RasGAP and total Akt signals, respectively; the results are presented as the fold induction over the nonstimulated control for each pair. These results show that vitreal VEGF-A preserves RV-induced indirect signaling downstream of activated PDGFRα by antagonizing vitreal PDGFs. (d) Model of the relationship between VEGF-A, PDGFs, and non-PDGFs in PVR. While PDGFs antagonize non-PDGF-mediated activation of PDGFRα, VEGF-A promotes non-PDGF-mediated activation of PDGFRα by antagonizing PDGFs. These observations suggest that VEGF-A promotes PVR by enhancing indirect activation of PDGFRα, which results in chronic signaling that drives cellular responses intrinsic to PVR pathogenesis (45).

PDGF-dependent signaling and cellular responses. Finally, neutralizing VEGF-A in vitreous restored the ability of vitreal PDGFs to activate PDGFRα, indicating that VEGF-A constitutes a substantial fraction of the PDGFRα inhibitory activity in vitreous. These discoveries underscore the importance of designing preventative therapies that not only target the growth factors involved in disease but also account for the functional relationships they have with each other.

In PVR vitreous, the preference of non-PDGFs over PDGFs for activation of PDGFRα appears to be due to VEGF-A. We previously reported that PDGFs antagonized non-PDGF-mediated activation of PDGFRα (45). In contrast, VEGF-A promotes non-PDGF-mediated activation of PDGFRα by antagonizing PDGF. The relationship between these three groups of agents is illustrated in Fig. 6d. Taken together, our findings predict that VEGF-A effectively induces a switch to indirect, chronic PDGFRα signaling, which drives the pathogenesis of PVR (45). This raises the intriguing idea that VEGF-A fosters PVR and that anti-VEGF-A could protect from this blinding disease. We are currently investigating this possibility.

It is also possible that the VEGF/PDGF relationship is important for maintaining physiology. Indirect activation of PDGFRα suppresses p53 (45) and thereby may enable cells to survive stressful situations, such as hypoxia (2, 32). For instance, a hypoxia-induced rise in the level of VEGF-A may switch the way the receptor signals from acute (via PDGFs) to chronic (via non-PDGFs) and thereby promote a fall in the level of p53, which would enhance the ability of cells to survive. Such transient, epigenetically driven suppression of p53 may be the physiological counterpart of permanent, genetic changes that reduce the level and/or function of p53 in the majority of human tumors (21, 46, 60).

Although the focus of the present study is the novel discovery that VEGF-A competes with PDGF to antagonize PDGFR-driven events, we also noted that VEGF-A activated PDGFRα (Fig. 5f). As a result, we may have underestimated the extent to which VEGF-A blocks PDGF-dependent activation of PDGFRα. However, this error is probably small because the extent of PDGFα activation by VEGF-A was very modest. Curiously, others report robust activation of PDGFRs by VEGF-A in mesenchymal stem cells (5); the difference in magnitude may relate to cell type, since our studies were performed with fibroblasts and epithelial cells.

VEGF-A was less capable of preventing PDGF-dependent binding to PDGFRα (Fig. 4a) than phosphorylation of PDGFRα (Fig. 3e). The data suggest that, in contrast to binding, which requires assembly of a stable dimer, PDGF-induced phosphorylation of PDGFRs may not require perfect or persistent dimerization. For instance, phosphorylation may persist within the relatively short time course of the activation assay regardless of whether the receptor stays dimerized. Which of these two parameters more accurately reflects the relevance of the VEGF-A/PDGF relationship to physiology and pathology remains an open question.

The inability of VEGF-A to effectively activate PDGFRα suggests that it does not bind in a way that results in activation of the receptor. Indeed, unlike PDGF, which dimerizes PDGFRα, several approaches failed to detect PDGFRα dimers after exposure to VEGF-A (Fig. 4c). Since ligand-induced receptor dimerization is a key component to activation of the kinases (9), it seems likely that VEGF-A failed to efficiently activate PDGFRα because it did not dimerize it properly. Binding PDGFRα without activating its kinase is a mode of interaction between members of the PDGF/VEGF family that was not known to exist.

Given the sequence homology and structural similarity within the VEGF/PDGF family (e.g., PDGF-C and -D exhibit higher structural similarity to VEGF-A than to other PDGF isoforms [18, 56]), we considered whether PDGFs competed with VEGF-A-dependent activation of VEGFR2. Our preliminary studies indicate that they did not (data not shown). One possible explanation involves Phe17 on the receptor binding face of VEGF-A, which is part of the N-terminal α-helix and a critical VEGFR2-binding determinant of VEGF-A (Fig. 3a) (50). The equivalent segment in PDGF-B not only lacks secondary structure, but the residues in this region are not thought to be involved in receptor binding (49, 51). Perhaps this dissimilarity excludes PDGF-B from binding VEGFR2.

The emerging picture is that VEGF-A can antagonize PDGF-dependent activation of PDGFRs, but not vice versa. This finding underscores that fact that interactions within the VEGF/PDGF family are highly selective. Members that are even more highly homologous than VEGF-A and PDGF-B can choose between PDGFR isoforms, e.g., PDGF-B, but not PDGF-A, binds to PDGFRβ (25, 59). We conclude that the ability of VEGF-A to competitively inhibit PDGF-dependent activation of PDGFRs is a previously unappreciated interaction within the high-fidelity VEGF/PDGF family.

REFERENCES

1. **Aiello LP, et al.** 1995. Suppression of retinal neovascularization in vivo by inhibition of vascular endothelial growth factor (VEGF) using soluble VEGF-receptor chimeric proteins. Proc. Natl. Acad. Sci. U. S. A. **92**: 10457–10461.
2. **Ak P, Levine AJ.** 2010. p53 and NF-κB: different strategies for responding to stress lead to a functional antagonism. FASEB J. **24**:3643–3652.
3. **Andrews A, et al.** 1999. Platelet-derived growth factor plays a key role in proliferative vitreoretinopathy. Invest. Ophthalmol. Vis. Sci. **40**:2683–2689.
4. **Bali E, et al.** 2003. IL-10 in vivo gene expression in a cell-induced animal model of proliferative vitreoretinopathy. Int. J. Mol. Med. **12**:305–310.
5. **Ball SG, Shuttleworth CA, Kielty CM.** 2007. Vascular endothelial growth factor can signal through platelet-derived growth factor receptors. J. Cell Biol. **177**:489–500.
6. **Banerjee S, et al.** 2007. Multiplex bead analysis of vitreous humor of patients with vitreoretinal disorders. Invest. Ophthalmol. Vis. Sci. **48**: 2203–2207.
7. **Baudouin C, et al.** 1993. Growth factors in vitreous and subretinal fluid cells from patients with proliferative vitreoretinopathy. Ophthalmic Res. **25**:52–59.
8. **Bowen-Pope DF, Ross R.** 1985. Methods for studying the platelet-derived growth factor receptor. Methods Enzymol. **109**:69–100.
9. **Burke CL, Stern DF.** 1998. Activation of Neu (ErbB-2) mediated by disulfide bond-induced dimerization reveals a receptor tyrosine kinase dimer interface. Mol. Cell. Biol. **18**:5371–5379.
10. Reference deleted.
11. **Campochiaro PA.** 1997. Mechanisms in ophthalmic disease: pathogenic mechanisms in proliferative vitreoretinopathy. Arch. Ophthalmol. **115**: 237–241.

12. **Canataroglu H, et al.** 2005. Interleukin (IL)-6, interleukin (IL)-8 levels and cellular composition of the vitreous humor in proliferative diabetic retinopathy, proliferative vitreoretinopathy, and traumatic proliferative vitreoretinopathy. Ocul. Immunol. Inflamm. **13**:375–381.

13. **Charteris DG.** 1998. Growth factors in proliferative vitreoretinopathy. Br. J. Ophthalmol. **82**:106.

14. **Cui JZ, et al.** 2007. Stage specificity of novel growth factor expression during development of proliferative vitreoretinopathy. Eye **21**:200–208.

15. **Dieudonne SC, et al.** 2007. Balance of vascular endothelial growth factor and pigment epithelial growth factor prior to development of proliferative vitreoretinopathy. Ophthalmic Res. **39**:148–154.

16. **El-Ghrably IA, Dua HS, Orr GM, Fischer D, Tighe PJ.** 2001. Intravitreal invading cells contribute to vitreal cytokine milieu in proliferative vitreoretinopathy. Br. J. Ophthalmol. **85**:461–470.

17. **Elner SG, et al.** 1995. Cytokines in proliferative diabetic retinopathy and proliferative vitreoretinopathy. Curr. Eye Res. **14**:1045–1053.

18. **Fredriksson L, Li H, Eriksson U.** 2004. The PDGF family: four gene products form five dimeric isoforms. Cytokine Growth Factor Rev. **15**:197–204.

19. **Gilbertson DG, et al.** 2001. Platelet-derived growth factor C (PDGF-C), a novel growth factor that binds to PDGF alpha and beta receptor. J. Biol. Chem. **276**:27406–27414.

20. **Glaser BM, Cardin A, Biscoe B.** 1987. Proliferative vitreoretinopathy: the mechanism of development of vitreoretinal traction. Ophthalmology **94**:327–332.

21. **Greenblatt MS, Bennett WP, Hollstein M, Harris CC.** 1994. Mutations in the p53 tumor suppressor gene: clues to cancer etiology and molecular pathogenesis. Cancer Res. **54**:4855–4878.

22. **Grinnell F, Ho CH, Lin YC, Skuta G.** 1999. Differences in the regulation of fibroblast contraction of floating versus stressed collagen matrices. J. Biol. Chem. **274**:918–923.

23. **Han D.** 2008. Proliferative vitreoretinopathy, p 2315–2324. Elsevier Saunders, Philadelphia, PA.

24. **Harada C, Mitamura Y, Harada T.** 2006. The role of cytokines and trophic factors in epiretinal membranes: involvement of signal transduction in glial cells. Prog. Retin. Eye Res. **25**:149–164.

25. **Hart CE, et al.** 1988. Two classes of PDGF receptor recognize different isoforms of PDGF. Science **240**:1529–1531.

26. **Himanen JP, Nikolov DB.** 2003. Eph receptors and ephrins. Int. J. Biochem. Cell Biol. **35**:130–134.

27. **Himanen JP, Saha N, Nikolov DB.** 2007. Cell-cell signaling via Eph receptors and ephrins. Curr. Opin. Cell Biol. **19**:534–542.

28. **Hinton DR, He S, Jin ML, Barron E, Ryan SJ.** 2002. Novel growth factors involved in the pathogenesis of proliferative vitreoretinopathy. Eye **16**:422–428.

29. **Ikuno Y, Kazlauskas A.** 2002. An in vivo gene therapy approach for experimental proliferative vitreoretinopathy using the truncated platelet-derived growth factor alpha receptor. Invest. Ophthalmol. Vis. Sci. **43**:2406–2411.

30. **Ikuno Y, Kazlauskas A.** 2002. TGFbeta1-dependent contraction of fibroblasts is mediated by the PDGFα receptor. Invest. Ophthalmol. Vis. Sci. **43**:41–46.

31. **Ikuno Y, Leong FL, Kazlauskas A.** 2000. Attenuation of experimental proliferative vitreoretinopathy by inhibiting the platelet-derived growth factor receptor. Invest. Ophthalmol. Vis. Sci. **41**:3107–3116.

32. **Jackson JG, Post SM, Lozano G.** 2011. Regulation of tissue- and stimulus-specific cell fate decisions by p53 in vivo. J. Pathol. **223**:127–136.

33. **Klinghoffer RA, Duckworth B, Valius M, Cantley L, Kazlauskas A.** 1996. Platelet-derived growth factor-dependent activation of phosphatidylinositol 3-kinase is regulated by receptor binding of SH2-domain-containing proteins which influence Ras activity. Mol. Cell. Biol. **16**:5905–5914.

34. **Kon CH, Occleston NL, Aylward GW, Khaw PT.** 1999. Expression of vitreous cytokines in proliferative vitreoretinopathy: a prospective study. Invest. Ophthalmol. Vis. Sci. **40**:705–712.

35. **La Heij EC, et al.** 2002. Basic fibroblast growth factor, glutamine synthetase, and interleukin-6 in vitreous fluid from eyes with retinal detachment complicated by proliferative vitreoretinopathy. Am. J. Ophthalmol. **134**:367–375.

36. **Laqua H, Machemer R.** 1975. Glial cell proliferation in retinal detachment (massive periretinal proliferation). Am. J. Ophthalmol. **80**:602–618.

37. **Lashkari K, Rahimi N, Kazlauskas A.** 1999. Hepatocyte growth factor receptor in human RPE cells: implications in proliferative vitreoretinopathy. Invest. Ophthalmol. Vis. Sci. **40**:149–156.

38. **Lee IG, Chae SL, Kim JC.** 2006. Involvement of circulating endothelial progenitor cells and vasculogenic factors in the pathogenesis of diabetic retinopathy. Eye **20**:546–552.

39. **Lei H, et al.** 2007. A potential role for PDGF-C in experimental and clinical proliferative vitreoretinopathy. Invest. Ophthalmol. Vis. Sci. **48**:2335–2342.

40. **Lei H, Kazlauskas A.** 2009. Growth factors outside of the platelet-derived growth factor (PDGF) family employ reactive oxygen species/Src family kinases to activate PDGF receptor alpha and thereby promote proliferation and survival of cells. J. Biol. Chem. **284**:6329–6336.

41. **Lei H, Rheaume MA, Kazlauskas A.** 2010. Recent developments in our understanding of how platelet-derived growth factor (PDGF) and its receptors contribute to proliferative vitreoretinopathy. Exp. Eye Res. **90**:376–381.

42. **Lei H, Rheaume MA, Velez G, Mukai S, Kazlauskas A.** 2011. Expression of PDGFRα is a determinant of the PVR potential of ARPE19 cells. Invest. Ophthalmol. Vis. Sci. **52**:5016–5021.

43. **Lei H, et al.** 2010. *N*-Acetylcysteine suppresses retinal detachment in an experimental model of proliferative vitreoretinopathy. Am. J. Pathol. **177**:132–140.

44. **Lei H, et al.** 2009. Growth factors outside the PDGF family drive experimental PVR. Invest. Ophthalmol. Vis. Sci. **50**:3394–3403.

45. **Lei H, Velez G, Kazlauskas A.** 2011. Pathological signaling via platelet-derived growth factor receptor α involves chronic activation of Akt and suppression of p53. Mol. Cell. Biol. **31**:1788–1799.

46. **Levine AJ.** 1997. p53, the cellular gatekeeper for growth and division. Cell **88**:323–331.

47. **Linggi B, Carpenter G.** 2006. ErbB receptors: new insights on mechanisms and biology. Trends Cell Biol. **16**:649–656.

48. **Mukherjee S, Guidry C.** 2007. The insulin-like growth factor system modulates retinal pigment epithelial cell tractional force generation. Invest. Ophthalmol. Vis. Sci. **48**:1892–1899.

49. **Muller YA, Christinger HW, Keyt BA, de Vos AM.** 1997. The crystal structure of vascular endothelial growth factor (VEGF) refined to 1.93 Å resolution: multiple copy flexibility and receptor binding. Structure **5**:1325–1338.

50. **Muller YA, et al.** 1997. Vascular endothelial growth factor: crystal structure and functional mapping of the kinase domain receptor binding site. Proc. Natl. Acad. Sci. U. S. A. **94**:7192–7197.

51. **Oefner C, D'Arcy A, Winkler FK, Eggimann B, Hosang M.** 1992. Crystal structure of human platelet-derived growth factor BB. EMBO J. **11**:3921–3926.

52. **Pastor JC.** 1998. Proliferative vitreoretinopathy: an overview. Surv. Ophthalmol. **43**:3–18.

53. **Pennock S, Kazlauskas A.** 2011. A novel strategy to develop therapeutic approaches to prevent proliferative vitreoretinopathy. Am. J. Pathol. **179**:2931–2940.

54. **Rahimi N, Kazlauskas A.** 1999. A role for cadherin-5 in regulation of vascular endothelial growth factor receptor 2 activity in endothelial cells. Mol. Biol. Cell **10**:3401–3407.

55. **Raines EW, Ross R.** 1985. Purification of human platelet-derived growth factor. Methods Enzymol. **109**:749–773.

56. **Reigstad LJ, Varhaug JE, Lillehaug JR.** 2005. Structural and functional specificities of PDGF-C and PDGF-D, the novel members of the platelet-derived growth factors family. FEBS J. **272**:5723–5741.

57. **Robbins SG, et al.** 1994. Platelet-derived growth factor ligands and receptors immunolocalized in proliferative retinal diseases. Invest. Ophthalmol. Vis. Sci. **35**:3649–3663.

58. **Ryan SJ.** 1993. Traction retinal detachment. XLIX. Edward Jackson Memorial Lecture. Am. J. Ophthalmol. **115**:1–20.

59. **Seifert RA, et al.** 1989. Two different subunits associate to create isoform-specific platelet-derived growth factor receptors. J. Biol. Chem. **264**:8771–8778.

60. **Toledo F, Wahl GM.** 2006. Regulating the p53 pathway: in vitro hypotheses, in vivo veritas. Nat. Rev. Cancer **6**:909–923.

61. **Waltenberger J, Claesson-Welsh L, Siegbahn A, Shibuya M, Heldin CH.** 1994. Different signal transduction properties of KDR and Flt1, two receptors for vascular endothelial growth factor. J. Biol. Chem. **269**:26988–26995.

62. **Zheng Y, et al.** 2003. Platelet-derived growth factor receptor kinase inhibitor AG1295 and inhibition of experimental proliferative vitreoretinopathy. Jpn. J. Ophthalmol. **47**:158–165.